Unravelling the future role of internal variability in South Asian near-surface wind speed

Cheng Shen¹, Hui-Shuang Yuan², Zhi-Bo Li¹, Jinling Piao^{3, 4, 5}, Youli Chang², Deliang Chen^{1, 6, *}

¹ Regional Climate Group, Department of Earth Sciences, University of Gothenburg, Gothenburg, Sweden

² Department of Atmospheric Science, Yunnan University, Kunming, China

³ State Key Laboratory of Earth System Numerical Modeling and Application, Institute of Atmospheric Physics, Chinese Academy of

10 Sciences, Beijing, China

⁴ Center for Monsoon System Research, Institute of Atmospheric Physics, Chinese Academy of Sciences, Beijing, China

⁵ College of Earth and Planetary Sciences, University of Chinese Academy of Sciences, Beijing, China

⁶ Department of Earth System Science, Tsinghua University, Beijing, China

Correspondence to: Deliang Chen (deliang@gvc.gu.se)

15

25

5

Abstract. Near-surface wind speed (NSWS) plays a critical role in water evaporation, air quality, and energy production. However, changes in NSWS over South Asia, a densely populated and climate-sensitive region, remain underexplored. This study aims to assess and quantify the uncertainties NSWS projections over South Asia, with a focus on internal variability. Using a 100-member large ensemble from the Max Planck Institute Earth System Model, we identified the Interdecadal Pacific Oscillation (IPO) as the dominant climate mode of internal variability affecting NSWS in the near future. Our results show that the positive phase of the IPO enhances regional westerly winds, leading to an increase in NSWS. Importantly, accounting for the influence of the IPO reduces projection uncertainty of NSWS by up to 8% in the near future and 15% in the far future. These findings highlight the critical role of internal variability, especially the IPO, in modulating regional NSWS projections. By narrowing uncertainties, this work supports improved planning for climate adaptation and wind energy development in South Asia.

1 Introduction

35

Near-surface wind speed (NSWS), observed at approximately 10 meters above ground level, is a crucial meteorological variable. As a key driver in the hydrological cycle, NSWS directly impacts water evaporation and runoff (Roderick et al., 2007). Additionally, NSWS is essential for air quality management by influencing the dispersion of atmospheric pollutants (Jacobson and Kaufman, 2006). Its importance extends to the renewable energy sector, particularly in wind energy generation, where fluctuations in NSWS can significantly affect the energy output of both onshore and offshore wind farms, as highlighted by recent research (Pryor and Barthelmie, 2021; Shen et al., 2024). In 2020, wind energy contributed 6.1% of global electricity generation, with projections indicating an increase in its share as the adoption of renewable energy grows to meet international goals for carbon emissions reduction and climate change mitigation (Antonini and Caldeira, 2021). External forcings that drive changes in NSWS include greenhouse gas emissions (Zha et al., 2021b), aerosols (Bichet et al., 2012), volcanic eruption (Shen et al., 2025), surface roughness related to vegetation changes (Vautard et al., 2010), as well as land use and land cover change (Minola et al., 2021; Zhang and Wang, 2021). Climate teleconnections such as the Atlantic Multidecadal Oscillation (AMO) (Li et al., 2024), Interdecadal Pacific Oscillation (IPO) (Shen et al., 2021a), El Niño-Southern Oscillation (Li et al., 2025), and the North Atlantic Oscillation (Minola et al., 2016) are significant modes of internal variability. Overall, these factors are typically categorized as either external forcings or internal variability drivers, with NSWS changes resulting from the combined influence of both (Wu et al., 2017; Zha et al., 2024; Andres-Martin et al., 2023).

The pressure gradient force predominantly controls changes in mean NSWS, with large-scale atmospheric circulation patterns playing a pivotal role at regional scales (Minola et al., 2023; Chuan et al., 2024; Zha et al., 2022; Zha et al., 2021a). Variations in these patterns are largely manifestations of internal variability, though external forcings like greenhouse gases and aerosols also exert some influence (Jiang and Zhou, 2023; Chen and Dai, 2024; Grant et al., 2025; Jiang et al., 2023; Liu et al., 2022; Xue et al., 2023). Understanding the degree to which NSWS changes are attributed to internal variability is essential for assessing the role of anthropogenic influences in past changes and for making reliable projections of future trends. However, our current knowledge in this area remains limited.

Previous studies have investigated long-term NSWS changes over South Asia (Jaswal and Koppar, 2013; Saha et al., 2017; Das and Roy, 2024). For example, South Asian NSWS experienced a significant decline from 1961 to 2008 (Jaswal and Koppar, 2013), with a more pronounced decrease along the eastern coast compared to the western coast (Saha et al., 2017).

However, only a few of these studies have attributed the observed changes to internal variability. Moreover, in model projections, NSWS shows considerable uncertainty in South Asia: Coupled Model Intercomparison Project phase 5 (CMIP5) models suggest an increase in NSWS on the eastern coast but a decrease on the western coast and northern regions by the end of the 21st century (Saha et al., 2017), while CMIP6 models project a decrease in NSWS over South Asia in the near future, followed by an increase (Shen et al., 2022a). These discrepancies emphasize the substantial uncertainties in projecting

future NSWS changes over South Asia.

Distinguishing the effects of internal variability from external forcing in NSWS changes using only observational data or a single simulation is challenging, as they provide just one realization (Shen et al., 2021b; Deng et al., 2024; Pryor et al., 2025). To isolate the signals of internal variability, we utilize large-ensemble simulations (LEs). These simulations share identical greenhouse gas emission scenarios and boundary conditions but differ only in initial condition disturbances (Deser et al., 2020). The multi-member ensemble mean (MMM) of the LEs represents the effects of external forcings, while differences among members reflect the impacts of internal variability (Mitchell et al., 2017; Li et al., 2019; Wu et al., 2021). In this study, we specifically use a 100-member Max Planck Institute Earth System Model (MPI-ESM), which has been compared its historical performance with observation-based data, and applied to project NSWS changes (Zha et al., 2021b; Shen et al., 2022a).

Therefore, our objectives are to (i) identify the leading mode of internal variability affecting near-future NSWS changes over South Asia and (ii) quantify the uncertainties of NSWS projections associated with internal variability. The remainder of this paper is structured as follows: Section 2 presents data and methods; Section 3 discusses the results; and the summary and discussion are provided in Section 4. These findings offer valuable insights for better understanding regional NSWS changes from the perspective of internal variability.

2 Material and Methods

2.1 Reanalysis data

75

To evaluate the ability of MPI-ESM to reproduce the historical NSWS trend over South Asia, we utilize several up-to-date reanalysis datasets. These include NSWS data from the Japanese Meteorological Agency (JRA55) (Kobayashi et al., 2015), which is considered the most representative of observed NSWS over India (Das and Baidya Roy, 2024); the National Meteorological Information Center of the China Meteorological Administration (CRA40), which has been shown to outperform other datasets for NSWS over China (Liu et al., 2023; Shen et al., 2022b); and the European Centre for Medium-Range Weather Forecasts atmospheric reanalysis fifth generation (ERA5) (Hersbach et al., 2020), a global reanalysis with the highest spatial resolution (Bell et al., 2021). All reanalysis datasets cover a common period from 1970 to 2020, except for CRA40, which spans from 1979 to 2020. To facilitate comparison, all reanalysis datasets have been bilinearly interpolated to a uniform spatial resolution of 1.5° x 1.5°.

2.2 Large-ensemble simulations

In this paper we selected the MPI-ESM LE primarily for its large ensemble size (100 members), which is well-suited for isolating internal variability. Other available LEs have smaller ensemble sizes (40–50 members), which may reduce their effectiveness in detecting internal variability (Milinski et al., 2020). The MPI-ESM has a horizontal spatial resolution of T63 (~1.9°) and 47 vertical layers extending up to 0.01 hPa in the atmosphere. The historical simulations of MPI-ESM span from 1850 to 2005, following the protocol established within the framework of CMIP5. The representative concentration pathway scenarios, RCP4.5 and RCP8.5, with radiative forcings increasing by 4.5 W/m² and 8.5 W/m², respectively, by 2100, are performed for the period from 2006 to 2099 (Maher et al., 2019). While data from 2006 to 2020 are technically part of the

RCP experiment, they no longer represent the future from today's perspective. Therefore, we define 2021 as the beginning of the future period, and designate 1970–2020 and 2021–2099 as the present and future periods, respectively. The individual members of the MPI-ESM ensemble differ only in their initial conditions (Bittner et al., 2016), with branching times for each member from the preindustrial control run detailed in (Maher et al., 2019). These "initial condition disturbances" refer to slight variations in the starting conditions of each member, introduced to capture a range of possible outcomes driven by internal variability(Deser et al., 2020; Phillips et al., 2014; Schneider et al., 2011).

2.3 Inter-member EOF

105

110

120

To identify the dominant spatial modes that account for the differences in NSWS trends across ensemble members, we employ an inter-member empirical orthogonal function (EOF) (Smith and Jiang, 1990; Hannachi et al., 2007). For inter-member EOF, the member index replacing the time index in a conventional EOF analysis. In other words, the decomposition is applied to an M×N matrix, where M represents the number of ensemble members (100 in this case), and N denotes the number of grid points over the South Asia region. Each row of the matrix contains the spatial pattern of NSWS trends for a single ensemble member. This analysis can help us yield the leading spatial modes that explain inter-member differences in NSWS trends, along with the associated principal component (PC) scores that characterize the magnitude of each mode across ensemble members.

2.4 Isolating external and internal forcing signals

Considering the differences among ensemble members of the MPI-ESM arising from random internal variabilities, the internal variability can be isolated by the deviations in each member from the MMM:

$$A(i) = A_{forced} + A_{internal}(i), i = 1,2,3 \cdots 100$$
 (1)

where A_{forced} is the MMM of the MPI-ESM, which denotes the response to external forcings. $A_{internal}(i)$ is the residual of the original A(i) minus the external forced response. $A_{internal}(i)$ varies among different members and shows the variability associated with internal variability.

2.5 IPO and AMO definitions

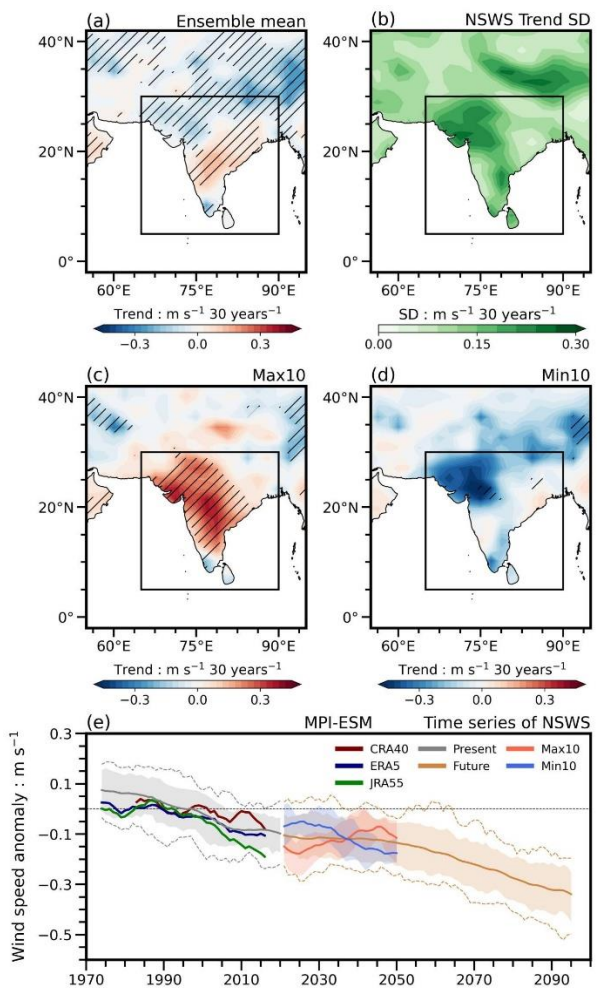
The climate teleconnection index used to represent the IPO is often derived using an EOF method applied to sea surface temperature (SST), as outlined by Mantua and Hare (2002). In this study, the IPO index is defined as the 9-year running mean of the PC score from the EOF of detrended annual SST over the North Pacific (20°N–70°N, 120°E–100°W). Similarly, the AMO index is defined as the 10-year running mean of detrended, annually averaged SST over the North Atlantic (0°N–60°N, 80°W–0°W) (Trenberth and Shea, 2006). As both the IPO and AMO indices are derived from detrended SSTs, they are inherently detrended and minimally affected by long-term global warming. For this analysis, both indices are calculated for each member in the LEs.

125 2.6 Quantifying the contributions of IPO/AMO to NSWS

The impacts of IPO are roughly extracted by removing the NSWS variations that are linearly related to the IPO index from 9-year running mean of NSWS, as:

$$NSWS(i,t) = r(i)_{NSWS,IPO} \times IPO(i,t) + NSWS_{non-IPO}(i,t), i = 1,2,3 \cdots 100$$
 (2)

where $r(i)_{NSWS,IPO} = \frac{\partial NSWS(i,t)}{\partial IPO(i,t)}$ is the regression coefficient of IPO index and the 9-year running mean NSWS within member *i* during 1974–2095. This extended period ensures statistical robustness by including multiple IPO cycles, thus effectively isolating the persistent, long-term influence of the IPO and reducing sampling uncertainty (Huang et al., 2020a; Jiang and Zhou, 2023). Thus, $r(i)_{NSWS,PDO} \times IPO(i,t)$ represents the IPO-related component of the NSWS over South Asia in the member *i* and the $NSWS_{non-IPO}(i,t)$ represents the IPO-independent NSWS component without the IPO-induced variations for each member (Fig. S1). Similar methods are also applied to study the contribution of AMO to NSWS. Following the timeframes selected in (Dreyfus et al., 2022), we set the 2021–2050 as the near-term and 2021–2095 as the full 21^{st} century to compare the contribution of IPO across different periods. Further details of the quantification method are provided in Figure S1.



140 Figure 1. Temporal NSWS changes over South Asia. Annual mean near-surface wind speed (NSWS) trends under the RCP8.5 scenario for (a) the 100-member ensemble mean of MPI-ESM, (b) inter-member standard deviation, (c) the mean trend of the 10 members with the highest increase in NSWS over

South Asia, and (d) the mean trend of the 10 members with the highest decline in NSWS over South Asia between 2021 and 2050. Slant hatching denotes trends that passed a significance test with P < 0.05. The box in (a) to (d) highlights the South Asia region (5°N-30°N, 65°E-90°E). (e) Time series of the 9-year running mean of NSWS anomalies (relative to the 1980-2010 mean). Purple, dark-blue, and green solid lines represent reanalysis data from CRA40, ERA5, and JRA55, respectively. Gray and brown solid lines represent the ensemble mean of all members of MPI-ESM for the present (1970-2020) and future (2021-2099), with light-gray and light-brown lines indicating the associated 5th and 95th percentiles. Orange and blue solid lines represent the ensemble mean of the ten simulations with maximum and minimum trends in NSWS. Dashed lines refer to the maximum and minimum ranges of MPI-ESM

150 3 Results

155

160

165

170

3.1 Present and near-future South Asian NSWS

To evaluate the ability of MPI-ESM in simulating NSWS, we compared its historical simulation over 1970–2020 with three reanalysis datasets. The MPI-ESM successfully reproduces the current slowdown of the NSWS trend, as seen in all reanalysis datasets, with comparable magnitudes of interdecadal variability (Fig. 1e). Note that the 2021–2099 data are based on the RCP8.5 scenario, whereas the 2006–2020 data follow the RCP4.5 scenario, aiming to reflect real-world conditions as closely as possible. Figure S2 further presents the mean NSWS trend over South Asia for each dataset. Specifically, the historical mean NSWS trends over South Asia are estimated to be -0.049, -0.037, -0.064, and -0.045 m s⁻¹ per 30 years for MPI-ESM, CRA40, ERA5, and JRA55, respectively. The results suggest that the decreasing trend of NSWS is generally captured by the MMM of MPI-ESM. Similarly, most regions in the reanalysis datasets also exhibit a reduction in NSWS. The differences between MPI-ESM and the reanalysis data may arise from that the ensemble mean tends to suppress internal variability, as such variability is random across individual members and can be averaged out. These findings indicate that the MPI-ESM large ensemble reasonably reproduces the historical NSWS trend, and that internal variability plays a significant role in shaping this trend over South Asia. Moreover, Figure S3 illustrates a good agreement in the 850 hPa wind climatology during the historical period between MPI-ESM and three reanalysis datasets. The model reproduces key largescale circulation features, such as the easterlies over the western Pacific and the westerlies over the Indian Ocean, supporting its credibility in simulating historical NSWS patterns. Under the high-emission scenario of RCP8.5, the externally forced annual NSWS in the MMM of MPI-ESM exhibits a relatively stable phase over South Asia in the near term, reflecting interdecadal variability. Notably, significant increases in NSWS are observed over the central and eastern coasts of India, contrasted by pronounced decreases over northern regions (Fig. 1a). The large standard deviation observed in the NSWS trends among members is comparable to the long-term trend (Fig. 1b), suggesting a substantial impact of internal variability on NSWS trends. Although the decreasing trend of NSWS in the MMM of MPI-ESM persists throughout the 21st century, significant uncertainty remains in near-term projections, as reflected by the large spread among members. The NSWS trends for this period range from -0.20 to 0.34 m s⁻¹ per 30 years, with the 5th to 95th percentile spread of -0.17 to 0.11 m s⁻¹ per 30 years.

175 To further quantify the impact of internal variability, we analyzed NSWS trends within two extreme groups: the ten members with the largest increases in NSWS (Max10) and the ten with the largest decreases (Min10). The Max10 group

displays pronounced increasing trends across most of South Asia (Fig. 1c), while the Min10 group primarily exhibits significant decreasing trends over northwestern South Asia (Fig. 1d). The average trend in the Min10 and Max10 groups is -0.18 m s^{-1} per 30 years and 0.14 m s^{-1} per 30 years, respectively. The diversity in NSWS changes between these two groups, despite identical external forcing, highlighting the significant role of internal variability in influencing South Asian NSWS.

180

185

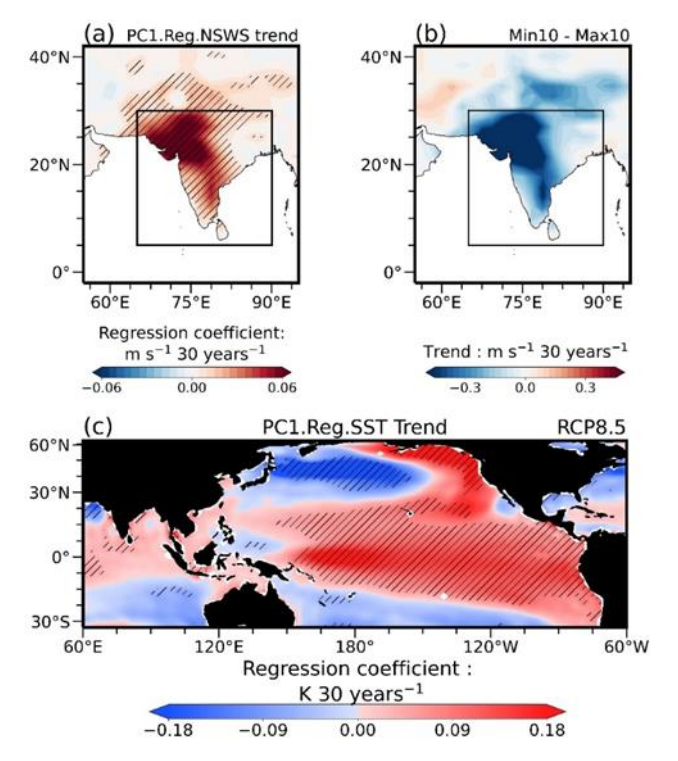


Figure 2. The leading inter-member EOF pattern of the NSWS trend over South Asia and the associated sea surface temperature trend under the RCP8.5 scenario between 2021 and 2050. (a) The first mode of an EOF analysis that applied to the NSWS trends over South Asia (5°N–30°N, 65°E–90°E) in MPI-ESM. Inter-member EOF based on a 100×N matrix, where N is the number of grid points over South Asia. (see Method). (b) The group differences between the mean trend of the ten members with the highest decline in NSWS over South Asia and the ten members with the highest increase. The box in (a) and (b) highlights the South Asia region. (c) The regression pattern between the PC score of (a) and the sea surface temperature trends of corresponding members. Slashes denote regions are significant at the 95% confidence level.

To identify the leading mode of internal variability affecting NSWS and its associated SST pattern, we performed an intermember EOF analysis. As shown in Fig. 2a, NSWS exhibits a uniform enhancement across South Asia, accounting for 54.6% of the total variance. This spatial pattern closely resembles the trend differences observed between the Max10 and Min10 groups (Fig. 2b), indicating that the EOF analysis successfully captures the leading mode of NSWS variability among members. Internal climate variability refers to the natural fluctuations of the climate system that occur in the absence of external forcing, arising from nonlinear dynamical processes intrinsic to the atmosphere, the ocean, and particularly the coupled ocean–atmosphere system, with ocean-atmosphere coupling playing a crucial role (Deser et al., 2010). The

regression coefficient between the leading PC of NSWS trends and the SST trends of corresponding members from 2021 to 2050 is shown in Fig. 2c. The regression analysis reveals a significant cooling trend over the North Pacific and a significant warming trend over the tropical central-eastern Pacific, resembling a classical IPO-like mode. This alignment highlights the IPO's role in modulating large-scale tropical atmospheric circulation, suggesting a strong link between surface and low-level tropospheric winds over South Asia. Moreover, to assess the robustness of these findings under different warming scenarios, we compared the results from the RCP4.5 scenario with those under RCP8.5, finding that the spatial patterns are quite similar (Fig. 3).

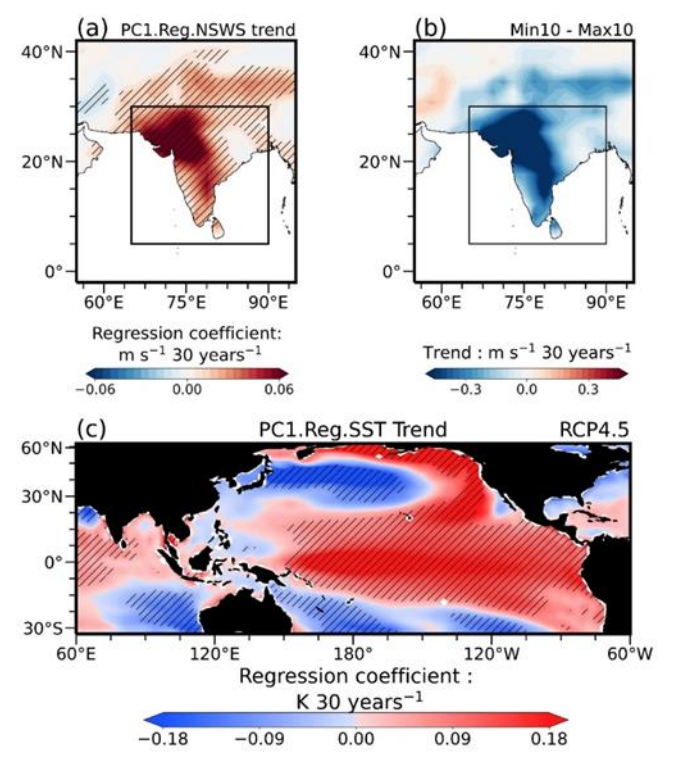


Figure 3. The leading inter-member EOF pattern of the NSWS trend over South Asia and the associated sea surface temperature trend under the RCP4.5 scenario between 2021 and 2050. (a)–(c) Same as in Figure 2, but for the representative concentration pathway 4.5 (RCP4.5).

3.2 Quantifying the contribution of IPO

200

210

215

Previous works have seldom explored the connection between low-level tropospheric winds and NSWS (Wu et al. 2017). However, changes in low-level tropospheric winds modify the vertical distribution of momentum, thereby leading to changes in wind shear between different atmospheric layers (Jacobson and Kaufman, 2006). Figure 4 illustrates the regression coefficient between the leading PC of NSWS trends and the trends in winds at 850 hPa and 10m. During the positive phase of the IPO, anomalous easterly winds over the tropical Indian Ocean are observed (Fig. 4a). This anomaly in tropical oceanic low-level tropospheric winds counteracts the climatological mean state (Fig. 4b), suggesting a weakening of the Walker Circulation. The resulting anomalous descending motion triggers anticyclonic circulation to the northwest of the Maritime

Continent, akin to the Gill response (Gill, 2007). The associated westerly winds, part of this anticyclone pattern near the Indian Ocean, enhance the climatological westerlies over South Asia. The MPI-ESM also provides data on surface meridional and zonal winds, allowing for exploration of the relationship between winds at 850 hPa and the surface. The spatial distributions of the regressed and climatological 10m winds (Figs. 4c and 4d) closely resemble those of the 850 hPa winds over South Asia (Figs. 4a and 4b), highlighting the consistency of atmospheric circulation changes within the region's lowest atmospheric layer.

To quantify the IPO's effect on NSWS changes over South Asia in the near future, we isolated the IPO-related NSWS changes by removing the NSWS changes linearly related to the IPO index in each member (see Section 2.6). Histogram analysis reveals a narrowing in the distribution of NSWS trends over South Asia after removing the IPO's effect, with the standard deviation in the members' trends decreasing by approximately 8%, from 0.09 to 0.08 m s⁻¹ per 30 years (Fig. 5a). Although modest, these reductions suggest that the uncertainty in NSWS trend projections over South Asia could be reduced by improving our ability to predict the IPO in the future. Applying this method to far-future projections for the 21st century (2021–2095) further confirms the sensitivity of these conclusions to the selected period and underscores the significance of long-term changes, which can be compared with inter-decadal variability in the near future. As expected, by eliminating the IPO's influence, projection uncertainty is significantly reduced by 15%, nearly double the reduction observed in the near future (Fig. 5b).

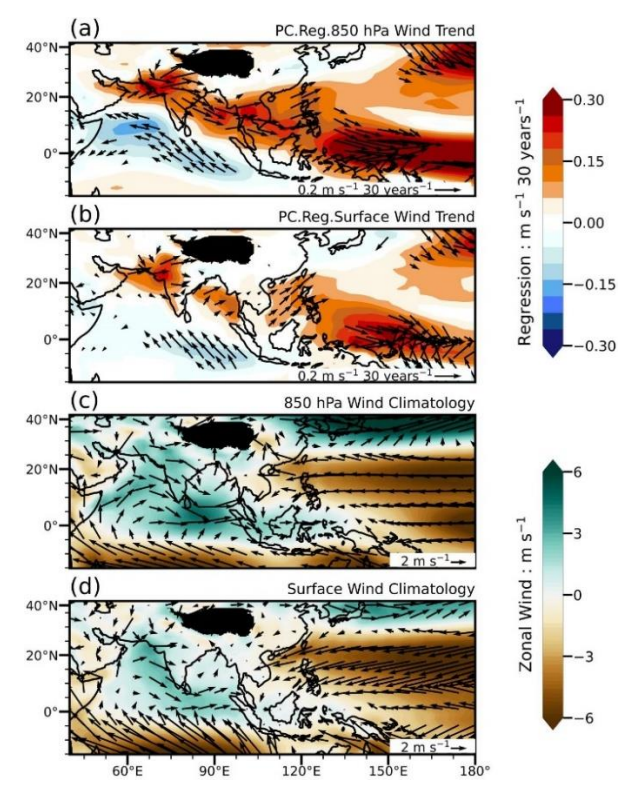


Figure 4. Large-scale circulations associated with the inter-member EOF and climatological circulations under the RCP8.5 scenario between 2021 and 2050. (a) The regression pattern between the PC score and the trends of corresponding members' zonal wind (shading) and wind (vector) at 850 hPa. Shading and vectors denote significance at the 0.10 level. (c) Climatological zonal wind (shading) and wind (vector) at 850 hPa from 2021 to 2050 across all members of MPI-ESM. (b) Same as (a), but for winds near the surface.

Notably, a recent study shows that over land in Asia, projection uncertainty is mostly dominated by model uncertainty, with internal variability accounting for around 20% of the total uncertainty (Zhang and Wang, 2024). This highlights the significant role of the IPO, whose contributions of 8% and 15% represent 40% and 75% of the internal variability in different future periods, respectively. This robust quantification supports the conclusion that NSWS projections are significantly affected by the IPO, with its influence growing and extending through the end of this century.

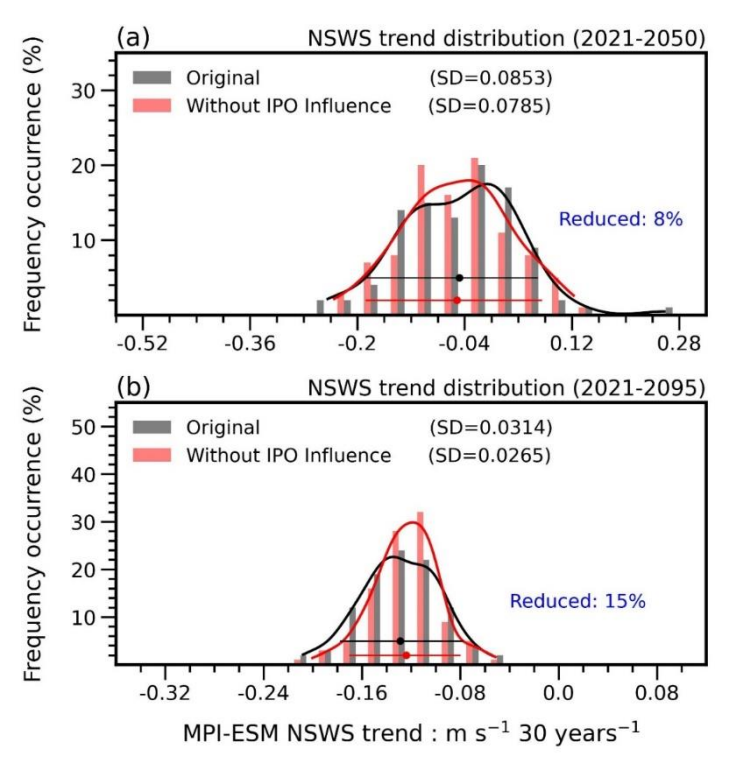


Figure 5. Histograms of the NSWS trend over South Asia in the future under the RCP8.5 scenario with and without the impact of the IPO. (a)

Histograms and fitted distribution lines of the area-averaged South Asian NSWS trend derived from the 100 MPI-ESM ensemble members from 2021 to

2050. The gray bars and black fitted curves show the frequency of the occurrence of NSWS trends, while the red bars and red fitted curves represent the
frequency of NSWS trends with the IPO's influence removed through linear regression against the IPO index in individual runs. (b) Same as (a), but for the
period from 2021 to 2095.

250 4 Conclusion and Discussion

235

240

In this study, LEs from the MPI-ESM are used to project future changes in NSWS over South Asia. We identify the IPO as the leading mode of internal variability affecting South Asian NSWS in the near future. A positive IPO phase enhances westerly winds over South Asia, resulting in increased NSWS. Furthermore, we quantify the influence of the IPO and find that removing its impact can reduce uncertainty in NSWS projections by approximately 8% in the near-term and 15% in the long-term. While these reductions may seem modest, they are important for regional planning, particularly in wind-sensitive sectors such as energy production, agriculture, and disaster risk management.

255

260

265

270

275

Our findings significantly improve the understanding of the relationship between internal variability and regional NSWS changes. Given the substantial IPO-related uncertainty, future studies should also consider other internal interdecadal climate variabilities that may affect NSWS. The AMO, for instance, is another important oscillation known to influence tropical atmospheric circulation (Zhang et al., 2019). However, our analysis using a similar quantification method reveals that the AMO's contribution to NSWS changes is minimal, further highlighting the dominant role of the IPO in modulating NSWS over South Asia in the near future (Fig. 6). The limited impact of the AMO on projected NSWS may partly be due to its longer oscillation period, which reduce its relevance over shorter time scales and may be masked by external forcings over longer periods. Additionally, the large geographic distance between the Atlantic and South Asia likely weakens the AMO's influence via teleconnection pathway, especially under strong external forcings.

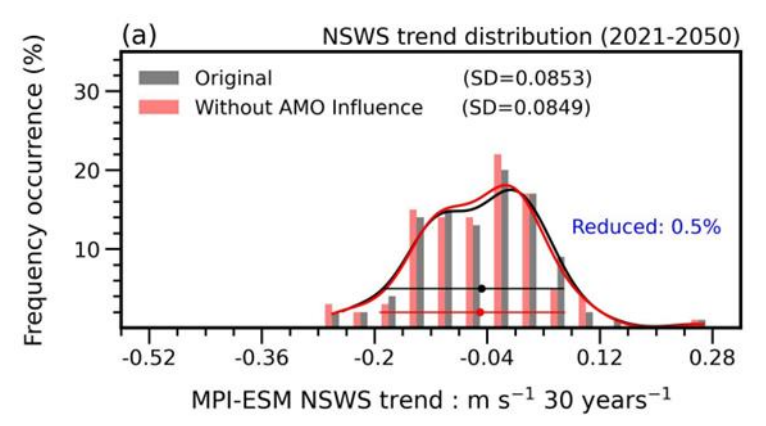


Figure 6. Histograms of the NSWS trend over South Asia under the RCP8.5 scenario with and without the impact of the AMO between 2021 and 2050. (a) Histograms and fitted distribution lines of the area-averaged South Asian NSWS trend derived from the 100 MPI-ESM ensemble members from 2021 to 2050. The gray bars and black fitted curves show the frequency of the occurrence of NSWS trends, while the red bars and red fitted curves represent the frequency of NSWS trends with the AMO's influence removed through linear regression against the AMO index in individual runs.

To date, few studies have systematically evaluated the ability of MPI-ESM, comparing to other models, to simulate the mechanisms by which the IPO influences atmospheric variables and associated SST variability in the western Pacific and Indian Oceans. Nonetheless, existing research has shown that MPI-ESM performs reasonably well in simulating key features of the Indian and East Asian summer monsoons (Guo et al., 2016). Similarly, studies by Prasanna et al. (2020) and Henley et al. (2017) indicate that CMIP5 models, including MPI-ESM, can generally reproduce the IPO and associated circulation features over South Asia. Furthermore, MPI-ESM has been applied in past studies to investigate IPO-related variability and

has demonstrated some skills in capturing its key spatial and temporal characteristics (Huang et al., 2020a; Huang et al., 2020b), lending confidence to its representation of internal variability in this study. However, Henley et al. (2017) also noted that many CMIP5 models underestimate the ratio of decadal-to-total SST variance, suggesting that the IPO's actual influence on variables like NSWS may be stronger than currently simulated.

The resolution of the LE used in this study may limit its ability to capture regional details over South Asia, which features complex terrain. Several areas for improvement remain and should be addressed in future research: (i) Future studies should incorporate additional LEs, with a sufficiently large ensemble size (Milinski et al., 2020), to enhance the robustness of these conclusions that currently rely heavily on a single model. (ii) The "hist-resIPO" experiment in CMIP6 (Zhou et al., 2016), which includes all forcings used in CMIP6 historical simulations but restores SST to model climatology plus observed historical anomalies in the tropical IPO domain, could offer deeper insights into the dynamic mechanisms through which IPO-related tropical SST's influence on regional NSWS changes. (iii) Improvements in IPO prediction, potentially achievable through the Decadal Climate Prediction Project in CMIP6, may enhance the reliability of future NSWS projections over South Asia (Zhou et al., 2016).

Although this study emphasize the role of the IPO in reducing NSWS projection uncertainty over South Asia, accurately predicting decadal IPO variations remains a major challenging (Pang et al., 2025). This limitation hampers the reliability of regional wind projections and highlights the need for improved prediction of internal climate variability. In addition, because our analysis is based on a single-model ensemble, the projection spread reflects internal variability only. Inter-model uncertainty, shown in other studies to exceed any single mode of internal variability, has yet to be assessed and should be a focus of future multi-model research. Finally, extreme wind events under a background of declining mean NSWS also merit attention, particularly as year-maximum NSWS events are projected to become more frequent in South Asia (Yu et al., 2024; Zha et al., 2023).

300 Financial support

305

310

320

This work is supported by Tsinghua University (100008001), the Swedish Formas (2023-01648), and the Swedish Research Council VR (2021-02163). Cheng Shen is also supported by the Sven Lindqvists Forskningsstiftelse, Stiftelsen Längmanska kulturfonden (BA24-0484), Stiftelsen Åforsk (24-707), and Adlerbertska Forskningsstiftelsen (AF2024-0069). Hui-Shuang Yuan is supported by the Innovation and Entrepreneurship Training Program for College Students of Yunnan University (S202310673266). Zhi-Bo is supported by the Swedish Formas (2020-00982).

Competing interests

The contact author declares that none of the authors have any competing interests.

Author contribution

All authors reviewed and revised the manuscript. C.S. and D.C planned and designed the study. C.S and H.S.Y conducted the visualization and analysis.

Acknowledgements

We thank Peter Pfleiderer and two anonymous reviewers for their insightful suggestions. This work is a contribution to the Swedish National Strategic Research Area MERGE. We would like to express our gratitude for the insightful discussion from our colleagues in the Regional Climate Group.

315 Code and data availability

All datasets used in this study are publicly available. ERA5 reanalysis data is available at Hersbach et al. (2020). CRA40 reanalysis data is available at Liu et al. (2023). JRA55 reanalysis data is available at Kobayashi et al. (2015). MPI-ESM reanalysis data is available at Maher et al. (2019). The Python script used for generating and analyzing are available on request.

References

- Andres-Martin, M., Azorin-Molina, C., Shen, C., Fernandez-Alvarez, J. C., Gimeno, L., Vicente-Serrano, S. M., and Zha, J.: Uncertainty in surface wind speed projections over the Iberian Peninsula: CMIP6 GCMs versus a WRF-RCM, Ann N Y Acad Sci, 1529, 101-108, 10.1111/nyas.15063, 2023.
- Antonini, E. G. A. and Caldeira, K.: Spatial constraints in large-scale expansion of wind power plants, Proc Natl Acad Sci U S A, 118, 10.1073/pnas.2103875118, 2021.
 - Bell, B., Hersbach, H., Simmons, A., Berrisford, P., Dahlgren, P., Horányi, A., Muñoz-Sabater, J., Nicolas, J., Radu, R., Schepers, D., Soci, C., Villaume, S., Bidlot, J. R., Haimberger, L., Woollen, J., Buontempo, C., and Thépaut, J. N.: The ERA5 global reanalysis: Preliminary extension to 1950, Quarterly Journal of the Royal Meteorological Society, 147, 4186-4227, 10.1002/qi.4174, 2021.
 - Bichet, A., Wild, M., Folini, D., and Schär, C.: Causes for decadal variations of wind speed over land: Sensitivity studies with a global climate model, Geophysical Research Letters, 39, 2012.
 - Bittner, M., Schmidt, H., Timmreck, C., and Sienz, F.: Using a large ensemble of simulations to assess the Northern Hemisphere stratospheric dynamical response to tropical volcanic eruptions and its uncertainty, Geophysical Research Letters, 43, 9324-9332, 10.1002/2016gl070587, 2016.
- Chen, X. and Dai, A.: Quantifying Contributions of External Forcing and Internal Variability to Arctic Warming During 1900–2021, Earth's Future, 12, e2023EF003734, 10.1029/2023ef003734, 2024.
 - Chuan, T., Wu, J., Zhao, D., Shen, C., Fan, W., and Jiang, H.: Asynchronous changes in terrestrial near-surface wind speed among regions across China from 1973 to 2017, Atmospheric Research, 300, 10.1016/j.atmosres.2024.107220, 2024.
- Das, A. and Baidya Roy, S.: JRA55 is the best reanalysis representing observed near-surface wind speeds over India, Atmos Res, 297, 10.1016/j.atmosres.2023.107111, 2024.
 - Das, A. and Roy, S. B.: JRA55 is the best reanalysis representing observed near-surface wind speeds over India, Atmospheric Research, 297, 107111, 10.1016/j.atmosres.2023.107111, 2024.
- Deng, K., Yang, S., Liu, W., Li, H., Chen, D., Lian, T., Zhang, G., Zha, J., and Shen, C.: The offshore wind speed changes in China: an insight into CMIP6 model simulation and future projections, Climate Dynamics, 62, 3305-3319, 10.1007/s00382-023-07066-1, 2024.
 - Deser, C., Phillips, A., Bourdette, V., and Teng, H.: Uncertainty in climate change projections: the role of internal variability, Climate Dynamics, 38, 527-546, 10.1007/s00382-010-0977-x, 2010.
 - Deser, C., Lehner, F., Rodgers, K. B., Ault, T., Delworth, T. L., DiNezio, P. N., Fiore, A., Frankignoul, C., Fyfe, J. C.,
- Horton, D. E., Kay, J. E., Knutti, R., Lovenduski, N. S., Marotzke, J., McKinnon, K. A., Minobe, S., Randerson, J., Screen, J. A., Simpson, I. R., and Ting, M.: Publisher Correction: Insights from Earth system model initial-condition large ensembles and future prospects, Nature Climate Change, 10, 791-791, 10.1038/s41558-020-0854-5, 2020.
 - Dreyfus, G. B., Xu, Y., Shindell, D. T., Zaelke, D., and Ramanathan, V.: Mitigating climate disruption in time: A self-consistent approach for avoiding both near-term and long-term global warming, Proc Natl Acad Sci U S A, 119, e2123536119, 10.1073/pnas.2123536119, 2022.
- Gill, A. E.: Some simple solutions for heat-induced tropical circulation, Quarterly Journal of the Royal Meteorological Society, 106, 447-462, 10.1002/qj.49710644905, 2007.
 - Grant, L., Vanderkelen, I., Gudmundsson, L., Fischer, E., Seneviratne, S. I., and Thiery, W.: Global emergence of unprecedented lifetime exposure to climate extremes, Nature, 641, 374-379, 10.1038/s41586-025-08907-1, 2025.
- Guo, Y., Cao, J., Li, H., Wang, J., and Ding, Y.: Simulation of the interface between the Indian summer monsoon and the East Asian summer monsoon: Intercomparison between MPI-ESM and ECHAM5/MPI-OM, Advances in Atmospheric Sciences, 33, 294-308, 10.1007/s00376-015-5073-z, 2016.
 - Hannachi, A., Jolliffe, I. T., and Stephenson, D. B.: Empirical orthogonal functions and related techniques in atmospheric science: A review, International Journal of Climatology, 27, 1119-1152, 10.1002/joc.1499, 2007.
- Henley, B. J., Meehl, G., Power, S. B., Folland, C. K., King, A. D., Brown, J. N., Karoly, D. J., Delage, F., Gallant, A. J. E., Freund, M., and Neukom, R.: Spatial and temporal agreement in climate model simulations of the Interdecadal Pacific Oscillation, Environ Res Lett, 12, 10.1088/1748-9326/aa5cc8, 2017.
 - Hersbach, H., Bell, B., Berrisford, P., Hirahara, S., Horányi, A., Muñoz-Sabater, J., Nicolas, J., Peubey, C., Radu, R., Schepers, D., Simmons, A., Soci, C., Abdalla, S., Abellan, X., Balsamo, G., Bechtold, P., Biavati, G., Bidlot, J., Bonavita,

- M., De Chiara, G., Dahlgren, P., Dee, D., Diamantakis, M., Dragani, R., Flemming, J., Forbes, R., Fuentes, M., Geer, A., Haimberger, L., Healy, S., Hogan, R. J., Hólm, E., Janisková, M., Keeley, S., Laloyaux, P., Lopez, P., Lupu, C., Radnoti, G., de Rosnay, P., Rozum, I., Vamborg, F., Villaume, S., and Thépaut, J. N.: The ERA5 global reanalysis, Quarterly Journal of the Royal Meteorological Society, 146, 1999-2049, 10.1002/qj.3803, 2020.
 - Huang, X., Zhou, T., Dai, A., Li, H., Li, C., Chen, X., Lu, J., Von Storch, J. S., and Wu, B.: South Asian summer monsoon
- projections constrained by the interdecadal Pacific oscillation, Sci Adv, 6, eaay6546, 10.1126/sciadv.aay6546, 2020a. Huang, X., Zhou, T., Turner, A., Dai, A., Chen, X., Clark, R., Jiang, J., Man, W., Murphy, J., Rostron, J., Wu, B., Zhang, L., Zhang, W., and Zou, L.: The Recent Decline and Recovery of Indian Summer Monsoon Rainfall: Relative Roles of External Forcing and Internal Variability, Journal of Climate, 33, 5035-5060, 10.1175/jcli-d-19-0833.1, 2020b.
- Jacobson, M. Z. and Kaufman, Y. J.: Wind reduction by aerosol particles, Geophys Res Lett, 33, 10.1029/2006gl027838, 380 2006.
 - Jaswal, A. and Koppar, A.: Climatology and trends in near-surface wind speed over India during 1961-2008, Mausam, 64, 417-436, 10.54302/mausam.v64i3.725 2013.
 - Jiang, J. and Zhou, T.: Agricultural drought over water-scarce Central Asia aggravated by internal climate variability, Nature Geoscience, 16, 154-161, 10.1038/s41561-022-01111-0, 2023.
- Jiang, J., Zhou, T., Qian, Y., Li, C., Song, F., Li, H., Chen, X., Zhang, W., and Chen, Z.: Precipitation regime changes in High Mountain Asia driven by cleaner air, Nature, 623, 544-549, 10.1038/s41586-023-06619-y, 2023.
 Kobayashi, S., Ota, Y., Harada, Y., Ebita, A., Moriya, M., Onoda, H., Onogi, K., Kamahori, H., Kobayashi, C., Endo, H., Miyaoka, K., and Takahashi, K.: The JRA-55 Reanalysis: General Specifications and Basic Characteristics, Journal of the Meteorological Society of Japan. Ser. II, 93, 5-48, 10.2151/jmsj.2015-001, 2015.
- Li, Z.-B., Xu, Y., Yuan, H.-S., Chang, Y., and Shen, C.: AMO footprint of the recent near-surface wind speed change over China, Environmental Research Letters, 19, 10.1088/1748-9326/ad7ee4, 2024.
 Li, Z., Sun, Y., Li, T., Ding, Y., and Hu, T.: Future Changes in East Asian Summer Monsoon Circulation and Precipitation Under 1.5 to 5 °C of Warming, Earth's Future, 7, 1391-1406, 10.1029/2019ef001276, 2019.
 - Li, Z. B., Sun, M., Shen, C., and Chen, D.: ENSO-driven seasonal variability in near-surface wind speed and wind power potential across China, Geophysical Research Letters, 52, e2025GL115537, 2025.
- potential across China, Geophysical Research Letters, 52, e2025GL115537, 2025.
 Liu, F., Gao, C., Chai, J., Robock, A., Wang, B., Li, J., Zhang, X., Huang, G., and Dong, W.: Tropical volcanism enhanced the East Asian summer monsoon during the last millennium, Nat Commun, 13, 3429, 10.1038/s41467-022-31108-7, 2022.
 Liu, Z., Jiang, L., Shi, C., Zhang, T., Zhou, Z., Liao, J., Yao, S., Liu, J., Wang, M., Wang, H., Liang, X., Zhang, Z., Yao, Y., Zhu, T., Chen, Z., Xu, W., Cao, L., Jiang, H., and Hu, K.: CRA-40/Atmosphere—The First-Generation Chinese Atmospheric
- Reanalysis (1979–2018): System Description and Performance Evaluation, Journal of Meteorological Research, 37, 1-19, 10.1007/s13351-023-2086-x, 2023.
 - Maher, N., Milinski, S., Suarez-Gutierrez, L., Botzet, M., Dobrynin, M., Kornblueh, L., Kröger, J., Takano, Y., Ghosh, R., Hedemann, C., Li, C., Li, H., Manzini, E., Notz, D., Putrasahan, D., Boysen, L., Claussen, M., Ilyina, T., Olonscheck, D., Raddatz, T., Stevens, B., and Marotzke, J.: The Max Planck Institute Grand Ensemble: Enabling the Exploration of Climate
- System Variability, Journal of Advances in Modeling Earth Systems, 11, 2050-2069, 10.1029/2019ms001639, 2019.
 Mantua, N. J. and Hare, S. R.: The Pacific Decadal Oscillation, Journal of Oceanography, 58, 35-44, 10.1023/a:1015820616384, 2002.
 - Milinski, S., Maher, N., and Olonscheck, D.: How large does a large ensemble need to be?, Earth System Dynamics, 11, 885-901, 10.5194/esd-11-885-2020, 2020.
- Minola, L., Azorin-Molina, C., and Chen, D.: Homogenization and Assessment of Observed Near-Surface Wind Speed Trends across Sweden, 1956–2013, Journal of Climate, 29, 7397-7415, 10.1175/jcli-d-15-0636.1, 2016.
 Minola, L., Reese, H., Lai, H. W., Azorin-Molina, C., Guijarro, J. A., Son, S. W., and Chen, D.: Wind stilling-reversal across Sweden: The impact of land-use and large-scale atmospheric circulation changes, International Journal of Climatology, 42, 1049-1071, 10.1002/joc.7289, 2021.
- Minola, L., Zhang, G., Ou, T., Kukulies, J., Curio, J., Guijarro, J. A., Deng, K., Azorin-Molina, C., Shen, C., Pezzoli, A., and Chen, D.: Climatology of near-surface wind speed from observational, reanalysis and high-resolution regional climate model data over the Tibetan Plateau, Climate Dynamics, 62, 933-953, 10.1007/s00382-023-06931-3, 2023.
 Mitchell, D., AchutaRao, K., Allen, M., Bethke, I., Beyerle, U., Ciavarella, A., Forster, P. M., Fuglestvedt, J., Gillett, N., Haustein, K., Ingram, W., Iversen, T., Kharin, V., Klingaman, N., Massey, N., Fischer, E., Schleussner, C.-F., Scinocca, J.,

Seland, Ø., Shiogama, H., Shuckburgh, E., Sparrow, S., Stone, D., Uhe, P., Wallom, D., Wehner, M., and Zaaboul, R.: Half a degree additional warming, prognosis and projected impacts (HAPPI): background and experimental design, Geoscientific Model Development, 10, 571-583, 10.5194/gmd-10-571-2017, 2017.
 Pang, B., Lu, R., Scaife, A. A., and Wang, L.: Increased resolution can reduce model biases in the Interdecadal Pacific

Oscillation, Environ Res Lett, 20, 10.1088/1748-9326/ade45a, 2025.

- Phillips, A. S., Deser, C., Alexander, M. A., and Smoliak, B. V.: Projecting North American Climate over the Next 50 Years: Uncertainty due to Internal Variability*, Journal of Climate, 27, 2271-2296, 10.1175/jcli-d-13-00451.1, 2014. Prasanna, V., Preethi, B., Oh, J., Kim, I., and Woo, S.: Performance of CMIP5 atmospheric general circulation model simulations over the Asian summer monsoon region, Global Planet Change, 194, 10.1016/j.gloplacha.2020.103298, 2020.
- Pryor, S. C. and Barthelmie, R. J.: A global assessment of extreme wind speeds for wind energy applications, Nature Energy, 6, 268-276, 10.1038/s41560-020-00773-7, 2021.
- Pryor, S. C., Coburn, J. J., Letson, F. W., Zhou, X., Bukovsky, M. S., and Barthelmie, R. J.: Historical and Future Windstorms in the Northeastern United States, Climate, 13, 10.3390/cli13050105, 2025.

 Roderick, M. L., Rotstayn, L. D., Farquhar, G. D., and Hobbins, M. T.: On the attribution of changing pan evaporation, Geophysical Research Letters, 34, 10.1029/2007gl031166, 2007.
- Saha, U., Chakraborty, R., Maitra, A., and Singh, A. K.: East-west coastal asymmetry in the summertime near surface wind speed and its projected change in future climate over the Indian region, Global and Planetary Change, 152, 76-87, 10.1016/j.gloplacha.2017.03.001, 2017.
 - Schneider, D. P., Deser, C., and Okumura, Y.: An assessment and interpretation of the observed warming of West Antarctica in the austral spring, Climate Dynamics, 38, 323-347, 10.1007/s00382-010-0985-x, 2011.
- Shen, C., Zha, J., Wu, J., and Zhao, D.: Centennial-scale variability of terrestrial near-surface wind speed over China from reanalysis, J Climate, 1-52, 10.1175/JCLI-D-20-0436.1, 2021a.

 Shen, C., Li, Z.-B., Liu, F., Chen, H. W., and Chen, D.: A robust reduction in near-surface wind speed after volcanic eruptions: Implications for wind energy generation, The Innovation, 6, 100734, 10.1016/j.xinn.2024.100734, 2025.
 - Shen, C., Li, Z. B., Yuan, H. S., Yu, Y., Lei, Y., and Chen, D.: Increases of Offshore Wind Potential in a Warming World,
- Geophys Res Lett, 51, 10.1029/2024gl109494, 2024.
 Shen, C., Zha, J., Li, Z., Azorin-Molina, C., Deng, K., Minola, L., and Chen, D.: Evaluation of global terrestrial near-surface wind speed simulated by CMIP6 models and their future projections, Annals of the New York Academy of Sciences, 1518, 249-263, 10.1111/nyas.14910, 2022a.
- Shen, C., Zha, J., Wu, J., Zhao, D., Azorin-Molina, C., Fan, W., and Yu, Y.: Does CRA-40 outperform other reanalysis products in evaluating near-surface wind speed changes over China?, Atmos Res, 266, 10.1016/j.atmosres.2021.105948, 2022b
 - Shen, C., Zha, J., Zhao, D., Wu, J., Fan, W., Yang, M., and Li, Z.: Estimating centennial-scale changes in global terrestrial near-surface wind speed based on CMIP6 GCMs, Environmental Research Letters, 16, 084039, 10.1088/1748-9326/ac1378, 2021b.
- Smith, J. M. W. C. and Jiang, Q.: Spatial Patterns of Atmosphere-Ocean Interaction in the Northern Winter, J Climate, 3, 990-998, 10.1175/1520-0442(1990)003%3C0990:SPOAOI%3E2.0.CO;2, 1990.

 Trenberth, K. E. and Shea, D. J.: Atlantic hurricanes and natural variability in 2005, Geophysical Research Letters, 33,
 - 10.1029/2006gl026894, 2006. Vautard, R., Cattiaux, J., Yiou, P., Thépaut, J.-N., and Ciais, P.: Northern Hemisphere atmospheric stilling partly attributed to
- an increase in surface roughness, Nature Geoscience, 3, 756-761, 10.1038/ngeo979, 2010. Wu, J., Zha, J., Zhao, D., and Yang, Q.: Changes in terrestrial near-surface wind speed and their possible causes: an overview, Clim Dynam, 51, 2039-2078, 10.1007/s00382-017-3997-y, 2017.
 - Wu, M., Zhou, T., Li, C., Li, H., Chen, X., Wu, B., Zhang, W., and Zhang, L.: A very likely weakening of Pacific Walker Circulation in constrained near-future projections, Nat Commun, 12, 6502, 10.1038/s41467-021-26693-y, 2021.
- Xue, D., Lu, J., Leung, L. R., Teng, H., Song, F., Zhou, T., and Zhang, Y.: Robust projection of East Asian summer monsoon rainfall based on dynamical modes of variability, Nat Commun, 14, 3856, 10.1038/s41467-023-39460-y, 2023.
 - Yu, Y., Li, Z., Yan, Z., Yuan, H., and Shen, C.: Projected Emergence Seasons of Year-Maximum Near-Surface Wind Speed, Geophys Res Lett, 51, 10.1029/2023gl107543, 2024.
 - Zha, J.-L., Shen, C., Wu, J., Zhao, D.-M., Fan, W.-X., Jiang, H.-P., Azorin-molina, C., and Chen, D.: Effects of Northern

- Hemisphere Annular Mode on terrestrial near-surface wind speed over eastern China from 1979 to 2017, Advances in Climate Change Research, 13, 875-883, 10.1016/j.accre.2022.10.005, 2022.
 - Zha, J., Shen, C., Zhao, D., Wu, J., and Fan, W.: Slowdown and reversal of terrestrial near-surface wind speed and its future changes over eastern China, Environmental Research Letters, 16, 034028, 10.1088/1748-9326/abe2cd, 2021a.
 - Zha, J., Shen, C., Wu, J., Zhao, D., Fan, W., Jiang, H., and Zhao, T.: Evaluation and Projection of Changes in Daily
- 475 Maximum Wind Speed over China Based on CMIP6, Journal of Climate, 36, 1503-1520, 10.1175/jcli-d-22-0193.1, 2023. Zha, J., Chuan, T., Wu, J., Zhao, D., Luo, M., Feng, J., Fan, W., Shen, C., and Jiang, H.: Attribution of Terrestrial Near–Surface Wind Speed Changes Across China at a Centennial Scale, Geophysical Research Letters, 51, 10.1029/2024g1108241, 2024.
- Zha, J., Shen, C., Li, Z., Wu, J., Zhao, D., Fan, W., Sun, M., Azorin-Molina, C., and Deng, K.: Projected changes in global terrestrial near-surface wind speed in 1.5° C–4.0° C global warming levels, Environmental Research Letters, 16, 114016, 10.1088/1748-9326/ac2fdd, 2021b.
 - Zhang, R., Sutton, R., Danabasoglu, G., Kwon, Y. O., Marsh, R., Yeager, S. G., Amrhein, D. E., and Little, C. M.: A Review of the Role of the Atlantic Meridional Overturning Circulation in Atlantic Multidecadal Variability and Associated Climate Impacts, Reviews of Geophysics, 57, 316-375, 10.1029/2019rg000644, 2019.
- Zhang, Z. and Wang, K.: Quantifying and adjusting the impact of urbanization on the observed surface wind speed over China from 1985 to 2017, Fundamental Research, 1, 785-791, 10.1016/j.fmre.2021.09.006, 2021.
 - Zhang, Z. and Wang, K.: Quantify uncertainty in historical simulation and future projection of surface wind speed over global land and ocean, Environmental Research Letters, 19, 054029, 10.1088/1748-9326/ad3e8f, 2024.
- Zhou, T., Turner, A. G., Kinter, J. L., Wang, B., Qian, Y., Chen, X., Wu, B., Wang, B., Liu, B., Zou, L., and He, B.: GMMIP (v1.0) contribution to CMIP6: Global Monsoons Model Inter-comparison Project, Geoscientific Model Development, 9, 3589-3604, 10.5194/gmd-9-3589-2016, 2016.